PHYSICAL REVIEW VOLUME 70, NUMBERS 3 AND 4 AUGUST 1 AND 15, 1946

Neutron Beam Spectrometer Studies of Boron, Cadmium, and the Energy Distribution from Paraffin*

JAMES RAINWATER AND WILLIAM W. HAVENS, JR.
Columbia University, New York, New York

(Received August 23, 1945)†

A slow neutron velocity selector has been developed for use with the Columbia University cyclotron. By the method of arc modulation, neutron production is usually confined to intervals of (10–200) microseconds out of a (1000–10,000) microsecond cycle. Neutrons slowed down in paraffin are detected by BF_3 proportional counters. Excellent collimation is obtained by using an extensive B_4C and Cd collimating system. Experiments were conducted principally at a 5.4-meter source detector distance. A special selector system counts all the neutrons detected and also selectively counts those detected in an adjustable timed interval after the cyclotron burst. The slow neutron energy distributions from paraffin "source" slabs were shown to be of a modified Maxwellian form with an asymmetrical high energy "tail." Data for the resonance absorption by Cd were well matched by a one-level Breit-Wigner formula having $E_0=(0.180\pm0.008)$ ev, $\Gamma=(0.112\pm0.006)$ ev, $\sigma_0=(7{,}800\pm800)\times10^{-24}$ cm²/atom. The results of measurements with several boron filters over the range of 0.01 ev to over 100 ev were well matched by the $1/v$ relation, $\sigma_B=(118\pm4)E^{-\frac{1}{2}}\times10^{-24}$ cm²/atom.

INTRODUCTION

THE variation with energy of the interaction of slow neutrons with nuclei supplies much of the detailed knowledge of the energy levels of these nuclei. Absorption bands are found at low neutron energies which give a picture of the levels of the compound nucleus in the vicinity of the binding energy of the neutron (8 Mev). When the energy of the neutron is in the thermal region, the wave-length of the neutron is of the same order of magnitude as the spacing between the atoms in molecules thus giving rise to interference and diffraction effects which offer important information concerning the structure of matter.

Experiments which have been carried out with slow neutrons usually depend on an arrangement in which fast neutrons produced in the course of nuclear disintegrations, such as take place in a cyclotron or in a radium-beryllium source, are slowed in paraffin or some other hydrogenous material to attain partial thermal equilibrium. Use of slow neutron detectors of the radioactive, ionization chamber, or proportional counter type, then permits absorption measurements to be made using the resultant energy distribution. These experiments have the disadvantage of using a wide distribution of neutron velocities. Although the distribution can be varied by controlling the temperature of the paraffin source and introducing absorbing filters such as Cd, the method does not give a sharply defined monochromatic neutron beam. In addition to the dependence of the energy distribution of the neutrons upon the temperature of the paraffin source there is also a dependence on the amount of paraffin used, the geometry of the system, and the energy of the fast neutrons used. These factors make difficult the proper evaluation of such experiments.

The use of resonance absorbers as detectors permits measurements to be made with neutrons of sharply defined energies corresponding to the resonance energies of the levels responsible for the slow neutron absorption.[1–4] When only one main absorption level is present, the energy of this level is usually determined by measuring the absorption cross section of a boron filter first for these resonance energy neutrons and then for the thermal energy neutrons removed by a cadmium filter. If boron is assumed to

* Submitted by James Rainwater in partial fulfillment of the requirements for the degree of Doctor of Philosophy in the Faculty of Pure Science, Columbia University, New York, New York. Publication assisted by the Ernest Kempton Adams Fund for Physical Research of Columbia University.

† The experimental work on this paper was completed prior to 1943, but publication was voluntarily withheld at the request of the Manhattan District until the date indicated.

[1] H. A. Bethe, Rev. Mod. Phys. 9, 113–161 (1937).
[2] H. B. Hanstein, Phys. Rev. 59, 489 (1941).
[3] W. J. Horvath and E. O. Salant, Phys. Rev. 59, 154 (1941).
[4] H. Feeny, C. Lapointe, and F. Rasetti, Phys. Rev. 61, 469 (1942).

TABLE I. Fundamental relations important in the measurements described in this paper.

$E\rightarrow$	1 Mev	0.1 Mev	0.01 Mev	1000 ev	100 ev	10 ev	1 ev	0.1 ev	0.01 ev	0.001 ev
V in meters/sec.	1.38×10^7	4.38×10^6	1.38×10^6	437,500	138,400	43,750	13,840	4375	1384	438
Microsec./meter	.0723	.229	.723	2.29	7.23	22.9	723	229	723	2286
Microsec./5.4 meters	.390	1.24	3.90	12.4	39.0	124	390	1235	3900	12,350
λ in A	.0003	.001	.003	.0091	.0286	.0905	.286	.905	2.86	9.05
Collisions required to cascade from 7 Mev	2	4	7	9	11	14	16	18	21	23
Assumed cm m.f.p.	4	1.3	.8	.7	.7	.7	.7	.4	.2	.2
Microsec. time required to cascade	.005	.01	.03	.06	.2	.7	2	4	9	20

absorb according to a $1/v$ law and if the effective energy of the thermal neutrons is assumed to be kT, the energy at resonance can be determined. Since the effective energy of the "thermal" neutrons used in such determinations is probably greater than kT (see below), this method usually gives too low a value for the resonance energy but a reasonably correct comparison of different levels.

The resonance absorption method can be used with high accuracy only in the special case in which there is a single resonance level involved. Also the properties of any element cannot be investigated over a continuously variable interval but can only be investigated at the energy values where suitable detection levels occur. These qualifications greatly limit the use of this method in determining the interesting properties of many of the nuclear levels.

Direct methods for obtaining monochromatic neutrons involve some sort of timing device whereby neutrons having different times of flight between source and detector can be separated. The times of flight of the neutrons, together with other pertinent data, are listed in Table I for different neutron energies.

When a steady source of neutrons is used, the only basic method possible is the use of a mechanical velocity selector. The first slow neutron velocity selector was the mechanical device of Dunning, Pegram, Fink, Mitchell, and Segré,[5] which was later improved by Fink.[6] This device used rotating disks with Cd sectors to pass bursts of slow neutrons from a radon beryllium source to a nearby ionization chamber detector similarly shielded by a second rotating disk with Cd sectors. The energy of the neutrons passed or discriminated against by the selector system depended on the separation of the disks and their speed of rotation and relative phase. Mechanical considerations limiting the possible speed of rotation confined the operation of the selector to the region of thermal energies. Because of the relatively large, fast neutron backgrounds inherent in such systems, the resolution could be made only moderately high. This method has one main advantage over other methods in that the time of starting of the slow neutron burst is definitely known within the limits of the resolution. This factor will be discussed later.

Another method was employed by Alvarez[7] with the Berkeley cyclotron. In this method the output of the cyclotron was modulated by supplying the plate voltage of the oscillator providing the D voltage with rectified but unfiltered 60-cycle high voltage. Since the efficiency of the cyclotron decreases rapidly with decreasing D voltage, most of the beam production was limited to the time when the D voltage was near the peak of the cycle. By placing the detector at different distances from the paraffin-surrounded target and counting the neutrons which arrived between the bursts at the source, the effects of neutrons of corresponding velocities could be observed. The arrangement employed was limited to energies below 0.025 ev. With half-wave rectification, the "on-time" was reduced to 20 percent of the cycle, which represents comparatively poor resolution, but eliminates the fast neutron background.

Experiments in which direct accelerating sources were modulated were conducted by Fertel, Gibbs, Moon, Thompson, and Wynn-

[5] Dunning, Pegram, Fink, Mitchell, and Segré, Phys. Rev. **48**, 704 (1935).

[6] G. A. Fink, Phys. Rev. **50**, 738 (1936).

[7] L. W. Alvarez, Phys. Rev. **54**, 609 (1938).

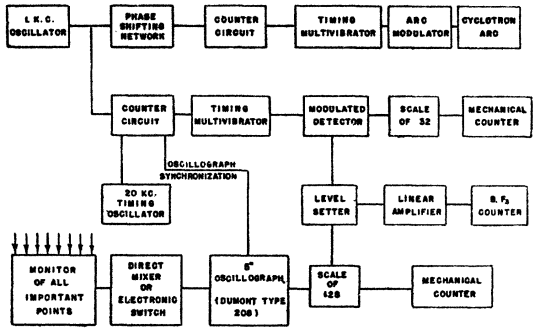

FIG. 1. Fundamental operating parts of the neutron beam spectrometer circuits.

Williams[8] and others, wherein the ion current was modulated and counts at a distant detector were recorded on an oscillograph as a function of time after the burst. The results of these experiments were not completely satisfactory because of the extremely low intensities obtained and because of the difficulties met with in the particular experiments conducted. This method has been used with good results by J. H. Manley, L. J. Haworth, and E. A. Luebke[9] who measured the lifetime of thermal neutrons in water and performed other experiments.

The present work is similar to that conducted by C. P. Baker and R. F. Bacher[10] using the Cornell cyclotron which was modulated by controlling the accelerating voltages of the ion source. Timed bursts of 50 to 100 microseconds duration could be produced with a 400-cycle repeat time. This work gave high resolution compared to the work previously mentioned as the "on-time" could be reduced to 8 percent of the total cycle. The distances employed, 1.5 and 3 meters, permitted experiments with neutron energies up to several electron volts and the resonance curves of several elements were studied. The accuracy of these measurements was limited by the low neutron intensities used, by background effects due to incomplete shielding from stray neutrons, and by the effect of the delayed emission of thermal neutrons from the thick paraffin "source" employed.

[8] Fertel, Gibbs, Moon, Thompson, and Wynn-Williams, Proc. Roy. Soc. **175**, 316 (1940).
[9] J. H. Manley, L. J. Haworth, and E. A. Luebke, Phys. Rev. **61**, 152 (1942).
[10] C. P. Baker and R. F. Bacher, Phys. Rev. **59**, 332 (1941).

The work described in this paper was undertaken to investigate more fully the possibilities of the modulated neutron-beam method with the Columbia cyclotron. The principal advantages of the present work include much higher intensities, better shielding from stray neutrons, thinner paraffin sources to minimize the uncertainty in the time of emission of neutrons from the paraffin, greater working distances, and, therefore, effectively higher resolution. Also, a more complete and flexible electronic control of the timing system was obtained over a wide range of neutron energies.

APPARATUS DESCRIPTION

Neutron Source

The neutron bursts are produced by modulating the accelerating voltage on the arc of the cyclotron. Arc currents of 1 to 2 amperes rise and fall in times shorter than 5 microseconds. The arc is modulated by a bank of 12 type 6L6 tubes which is controlled by appropriate pulses from the modulation system. The width of the pulses can be varied continuously from less than 10 microseconds to 1000 microseconds out of a total cycle period of 1000 to 10,000 microseconds. The cyclotron is operated with an internal beryllium target on a probe placed for maximum stability in a position corresponding to a beam of about 8-Mev energy. Instantaneous beam currents utilized are of the order of 50 to 200 microamperes which give fairly high neutron intensities.

Timing Circuits

The fundamental arrangement employed in controlling the cyclotron and detector is shown in Fig. 1. A thousand-cycle oscillator of the "transitron" type was calibrated by using a scaling circuit and a clock to determine the fundamental timing frequency. The output of this oscillator was divided into two parts.

One part was fed to a circuit which converted the sine wave output to a square wave. This square wave then operated a counter circuit which could be set to respond to any number of cycles from 1 to 10 to give a corresponding frequency reduction in the fundamental timing cycle. This gave flexibility in changing the

timing cycle, so that the optimum value could be used for any experiment performed. The output of this counter circuit triggered a special multivibrator circuit. This produced the fundamental modulation pulse which could be varied from 10 to 1000 microseconds in width. The output of this circuit activated the "level-setters" on the detectors so that only neutrons detected within the duration of the pulse would be recorded as "timed counts."

The other part of the oscillator output was fed to a phase-shifting condenser output. The sine wave could be shifted in phase continuously by any desired amount. The phase shift was linear with angle of rotation of the phase-shifting condenser with one revolution of the phase-shifting condenser corresponding to 1000 microseconds, or one cycle, phase shift in the wave. The output of this condenser went to another counting circuit and timing multivibrator. The output of this timing multivibrator was then fed to a low impedance power output circuit, then over a line to a power amplifier which was in series with the exciting voltage generator of the arc of the cyclotron.

Arc Modulation

To investigate the sharpness of the arc modulation, an amplifier circuit was arranged to respond only to current pulses through the arc so the current pulse in the arc circuit could be studied on an oscillograph screen. These pulses were as sharp as could be expected in view of the amplifier circuit constants. The voltage pulses to "fire" the arc tended to produce an opposite effect so that when there was no arc, negative pulses were seen on the screen in place of the normal positive pulses. When the filament current was increased to the value where the arc would strike, the current pulses reversed the direction of the pulses to a positive value several times the previous size. This afforded an excellent check on the operation of the arc. The pulse observed rose and fell in about 5 microseconds. The limitation was probably, to a considerable extent, in the frequency response of the amplifier itself.

The time required for the voltage pulse to the arc to rise was determined by the sharpness of the grid signal applied to the power amplifier and by the rate at which the initial current could charge the r-f filtering condenser on the arc. Since this filtering capacitance was 0.004 microfarad and the initial currents were of the order of 1 ampere, the time required to charge the condenser to the operating voltage of the arc, 200 volts, should be less than 1 microsecond. The rate at which the voltage pulse decreased was determined by the rate at which the 0.004 microfarad condenser was discharged when the tubes ceased conducting. A 500-ohm resistor in parallel with the arc reduced this time to less than 5 microseconds. The manner in which the arc current followed the voltage pulse was less definite, but the time of firing was less than 5 microseconds, and probably less than one microsecond.

The arc source used was an enclosed capillary type, fairly well shielded from the main r-f voltage on the dees, so that the stopping of the ion production should be quite clean. Supplementary sources of ions should be relatively ineffective. A study of the results shows there can be no very large error from this source. This is best shown by the experimental resolution curve of Fig. 3 together with the fact that the neutron production dropped to zero when no modulation pulses "fired" the arc.

Monitoring of Circuit Operation

In order to keep check on the operation of the circuits, a buffer triode was attached to each essential point of the circuit. A special switching

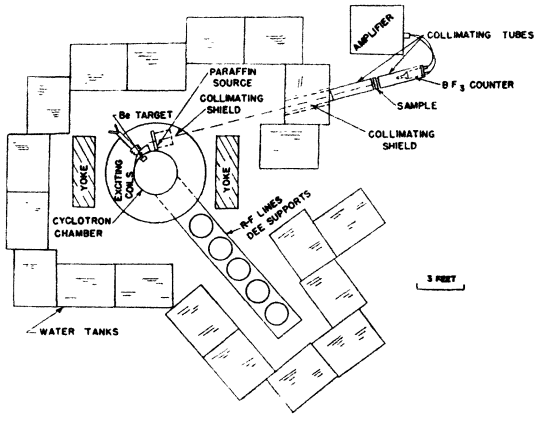

FIG. 2. Room plan showing the cyclotron, the water tank shielding the collimating system, and the slow neutron "source," sample, and detector positions.

arrangement permitted—(a) direct examination of the wave form at any point; (b) the direct addition of two wave forms in a mixer circuit; (c) the simultaneous observation of three points by use of two synchronized electronic switches of special design.

Timing Measurements

A 20-kilocycle transitron oscillator synchronized to the same point from which the oscillograph synchronization was obtained permitted all timing measurements to be made directly in units of cycles or fractions of cycles of the 20-kilocycle wave. A 5″ Dumont Type 208 oscillograph was used for all measurements. Parts of the pattern could be expanded to give 50 microseconds-per-inch spread so that measurements could be made to 5 microseconds or better.

Floor Plan of the Cyclotron Enclosure

The geometry of the paraffin and the collimating arrangement is shown in Fig. 2 for the work at 5.40 meters distance between the effective slow neutron source and the detector. The cyclotron chamber is located between the 36-inch diameter pole pieces of the magnet. The target was a piece of beryllium on a probe placed about 15″ from the center of the chamber.

Slow Neutron Sources

The effective source of slow neutrons was a vertical paraffin slab placed on the case of the magnet coils to slow down the fast neutrons produced at the target. While the thickness of the paraffin slab could be varied to give the best neutron distribution for a given experiment, other considerations made it more desirable to use one standard thickness. Experiments investigating the relative slow neutron intensity from the source slab as a function of slab thickness had indicated that a maximum was obtained for a 4.5-cm slab while with cadmium over the slab the maximum occurred for a 2.5-cm slab. Since the consideration of the delayed emission of thermal neutrons (see below) suggested as thin a source as possible, a compromise value was employed.

For most of the experiments a source consisting of a 2.6-cm thickness of paraffin in a 0.25-in. thick plywood box was used. Because of its low density and hydrogen content the total 0.5-in. thickness of plywood present was equivalent to only about 0.3-cm paraffin.

Collimation and Shielding

The collimation and shielding employed are shown in Fig. 2. The cyclotron was surrounded by thick water tanks to reduce the external radiation to a minimum. In one of these tanks a central slot was provided through which the collimated path was taken. A B_2O_3 cadmium collimating shield was placed in the slot and the space to the sides was filled in with boxes containing a 30 percent boric acid, 70 percent paraffin mixture. A similar small collimating section was placed in front of the paraffin slab to reduce the effect of neutrons scattered from the water tanks.

The final collimation for each detector was provided by two 36-inch collimating tubes in a line placed outside the enclosure. These tubes were 5-inches O.D. and 3.25-inches I.D. lined with cadmium. The 0.75-inch thickness between the inner and outer walls was filled with dried boron oxide in the first tubes and with dried boron carbide in the second tubes containing the counters. The counters were mounted in brass tubes and the electrical connections were brought out through cadmium shields. In this manner excellent shielding from stray neutrons was obtained.

In order to investigate the completeness of the collimation the following experiments were carried out. Thick cadmium (0.43 g/cm^2) was placed between the collimating tubes in the sample position and a reduction of total intensity from 100 to 7 in arbitrary units was obtained. When the timing was set for the peak of the neutron distribution coming from paraffin, the intensity of the timed neutrons was reduced from 100 to 0.79 when Cd was placed over the source and was reduced from 100 to 0.43 when Cd was placed over the tube (see Fig. 8) thus showing that essentially all the neutrons counted came from the slab of paraffin which served as the effective source. A thick boron carbide filter placed in the sample position reduced the total intensity from 100 to 1, illustrating the effective-

ness of the shielding obtained with the collimating tubes and the smallness of the total fast neutron background.

Detection

Proportional counters normally filled to a pressure of 30 cm of BF_3 were used to detect the neutrons. The counters were enclosed in an envelope of soft glass of low boron content with a copper screen cylinder 5 cm in diameter and 20 cm long as the negative electrode and a tungsten wire (0.01 cm diameter) as the positive electrode. The proportional region of these counters was very broad. They could be used anywhere between 2400 and 3500 volts. The "Geiger region" at which the counter responded equally to beta-particles was reached at about 4000 volts.

Proportional counters have several advantages over ionization chambers in this type of work in that (a) the pulses are usually of shorter duration; (b) the amplification required is much less, and, therefore, they are much less subject to r-f and other types of pick-up; (c) there is less response to gamma-radiation. The disadvantages of a proportional counter include the somewhat greater non-uniformity of pulse sizes, the tendency of the gas amplification to drift because of temperature changes in the counter, and the lower sensitivity.

The output of the proportional-counter, linear-amplifier was fed to a level-setter which was set at approximately $\frac{1}{4}$ the height of the highest neutron pulses, to insure that only neutrons were counted. This was further tested by timed counts with a Cd filter in the region of 200 microseconds/meter.

The change in gas amplification due to temperature changes was found to be very slow when the counters were compared with each other and with ionization chamber systems around the cyclotron. Any error due to this source was eliminated entirely by referring the number of neutrons counted in a timed interval to the total number of neutrons counted in the total interval of time. In this manner a change in the efficiency of counting would represent an equal change in both values and cancel. Since such changes are relatively slow, this is not considered a serious source of error even when comparison measurements with two counters were made to obtain the total cross section.

The output of the proportional counter was fed to a twin channel 5-stage linear amplifier. Previous work with proportional counters had shown that if the low frequency response of the amplifiers was maintained the pulse would rise sharply and then gradually drop again to zero. Since the effective on-time of the detector modulation also includes the counter pulse width above the level-setter height, it was desirable to narrow the pulse width as much as possible. To reduce the low frequency response of the amplifier the input resistor of the first tube was reduced to 25,000 ohms and the time constants of the coupling of successive stages were kept small. Inverse feedback by pairs was used to make the total gain of the amplifier almost independent of line voltage and other fluctuations. The fifth stage of the amplifier used a type of 6L6 tube to provide low impedance output. The output of the amplifier was fed over low impedance transmission lines to the cyclotron control room some distance away where the counting circuits and the modulation equipment were operated.

CALIBRATION OF THE INSTRUMENT

When the results of experiments performed with the instrument are to be evaluated, it is first necessary to evaluate all the factors and uncertainties inherent in the instrument and the method which will influence the results. The factors involved here are discussed below.

1. Path Length for Timed Flight

The distance measured was from the front surface of the paraffin source slab to the center of the proportional counter. If the effective starting point were some distance below the paraffin surface, this would represent a source of error. For transmission measurements at 5.4 meters a source consisting of 2.6-cm paraffin in a box of $\frac{1}{4}''$ plywood was used so this effect would be small.

The effect of the 20-cm counter length is to broaden the resolution of the instrument. For a 5.4-meter path this effect gives a maximum uncertainty in a velocity measurement of ± 1.85 percent. When the uncertainty is converted to a

time of flight uncertainty, this represents a total extra resolution broadening of 3.7 percent of the measured time of flight. Since the probability of detecting a slow neutron directed along the length of the counter is only a few percent, the displacement of the effective center of the counter towards the near end is always negligible.

2. Measurement of the Time Interval Between the Cyclotron and Detector On-Time Intervals

The frequency of the 1000-cycle oscillator establishing the fundamental timing was measured occasionally with a scaling-circuit and a clock and was seldom found in error more than 0.1 percent. The timing measurements were in terms of a synchronized 20-kc oscillator and were probably known always to within 5 microseconds.

3. Over-All Time Lag of the System

The effective time-of-flight of the neutrons from the paraffin source to the detector will be less than the measured spacing between the cyclotron and detector on-time intervals because of time lags in the neutron production and detection. First there is a time interval of the order of 5–10 microseconds required for the deuterons to be accelerated in the cyclotron before striking the target. Then a negligible time is required for the neutrons to slow to energies of the order of a few electron volts and escape (see Table I). Since a detected neutron will be counted in a timed interval if the resultant pulse height is above the level-setter position during any portion of the detection interval there will also be an effective detection time lag, from the time the neutron is captured by a boron nucleus in the counter to the time when the resultant pulse reaches the center of its interval above the level-setter height.

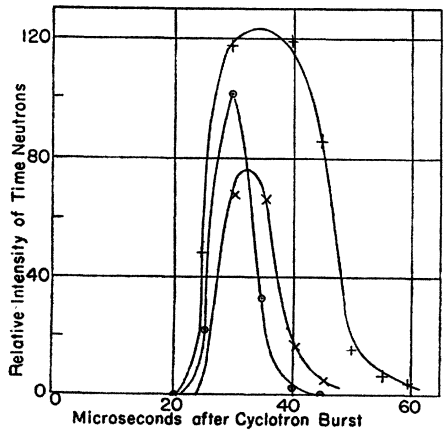

FIG. 3. Experimental resolution curve. Data taken 8 cm from the paraffin "source." O = counter in B_4C shield with a pulse sharpener. + = counter in B_4C shield without the pulse sharpener. × = with Cd shielding with a pulse sharpener.

The over-all time lag of the instrument may be directly determined by measuring the slow neutron intensity from the paraffin source slab as a function of cyclotron and detector on-time spacing with the detector near the source. The results of these measurements are shown in Fig. 3.

The counter was mounted in a cylindrical B_4C-Cd shield with an opening in the side facing the source slab. In one set of measurements a B_4C-Cd plug was placed in the slot to eliminate all but the highest energy slow neutrons. In the second set the plug was removed and Cd filtration was employed. Although the counter was placed as close to the source as possible in these measurements, the effect of 8-cm distance from the front of the source to the counter axis shows up as a 5-microsecond shift. This represents the time of flight of the slower neutrons above the Cd cut-off region over this short distance.

In two of the measurements a special pulse sharpening circuit was employed to minimize the effect of the pulse width when the cyclotron and detection on-time were reduced to an extreme minimum. Comparisons with and without the sharpening circuit clearly show the effect of the pulse width on the effective resolution. In the other experiments described in this paper this pulse sharpener was not employed as such extreme resolution was not required. Figure 3 shows better than any other experiment the sharpness of the source modulation starting and stopping.

When the sharpening circuit was not employed, the resulting intensity function appeared flat on top rather than triangular as only the pulse width was important. When the source and detection on-time widths are equal, the resolution function is more nearly the usual triangular shape.

From Fig. 3 it is seen that the basic delay time is 30 microseconds to which must be added half the pulse width. Accordingly 35 microseconds was deducted from all measurements when the sharpening circuit was not employed.

4. Thermal Emission Delay

Neutrons slowed in paraffin will continue to suffer collisions in the paraffin until they escape or are captured. This results in a continued emission of thermal neutrons from the paraffin slab for a considerable time after the production of fast neutrons has ceased. This delayed emission will decay with a mean life for decay determined by the thickness of the paraffin for diffusion and by the mean lifetime for capture of a neutron in paraffin of about 180–200 microseconds. Applying simple diffusion theory to this problem it is found that the diffusion of thermal neutrons from the source should roughly be proportional to the square of the paraffin thickness for thin samples and limited by the mean life for capture for thicker slabs. Using probable values for the diffusion coefficient and the mean life for capture in paraffin the predicted mean lives for decay for the two sources measured have been calculated.

For the main measurements a paraffin source consisting of 2.6 cm of paraffin enclosed in a box of $\frac{1}{4}$-inch thick plywood was used. The effective source thickness for diffusion, after the effect of the plywood and the necessary zero correction at edges were considered, was taken as 3.2 cm. The predicted mean life for decay for this thickness was 43 microseconds. The second source used consisted of a 6.2-cm thickness of paraffin in a box of $\frac{1}{4}$-inch thick plywood corresponding to 6.8-cm effective diffusion thickness. The predicted mean life for decay from this thickness was about 100 microseconds.

In order to measure experimentally the effective decay time of the thermal emission from these slabs measurements were made with the counter next to the source. The collimating arrangement mentioned above was used with the opening next to the slab. After making these measurements it was at once apparent that the time required for the thermal neutrons to travel the few centimeters distance to the counter was sufficiently great to render the results meaningless.

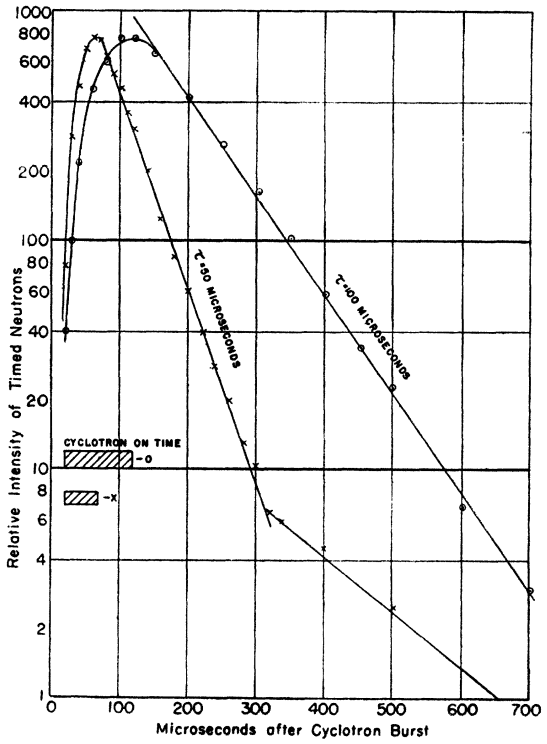

FIG. 4. Thermal neutron delayed emission from paraffin "source" slabs. Data taken next to the source with a tiny BF_3 counter. $\times$ = 2.6 cm thick paraffin in a box of $\frac{1}{4}$" thick plywood. $\circ$ = 6.2 cm thick paraffin in a box of $\frac{1}{4}$" thick plywood.

To reduce the path length still farther a tiny BF_3 counter 1 cm in diameter was used in contact with the slab. The results of these measurements are shown in Fig. 4. For the measurements with the thin source a cyclotron on-time of 50 microseconds and a detector on-time of 15 microseconds were employed. There was an exponential rise in intensity during the cyclotron on-time and then an exponential decay of intensity after production had ceased. Although a decay time of 50 microseconds seems clearly indicated from Fig. 4, the results of different measurements gave values between 43 and 50 microseconds. In these and other measurements with thinner slabs there seemed evidence that the measured time tended to be too large so a value of (45 ± 5) microseconds was selected as the effective decay time for this source.

The measurement of the thicker source gave a more extended straight line logarithmic plot with a decay time of 100 microseconds. This value

agrees exactly with the predicted value but differences obtained in different measurements indicate that this value should be expressed as (100 ± 10) microseconds.

Timing Correction

As a result of the factors mentioned above a deduction of 35 microseconds was made from all time-of-flight measurements. In the thermal energy region an additional deduction was made equal to the mean decay time for the emission of thermal neutrons from the source. In the intermediate region a fractional deduction was made as an approximate method of bridging the gap between the thermal and higher energy regions. Fortunately, as may be seen from Figs. 6 and 7, this transition is relatively abrupt on a time-of-flight basis.

Resolution Width

The total resolution width for times-of-flight below the thermal region was taken as the sum of the cyclotron and detector on-times, the detector pulse width, and 3.7 percent of the corrected time-of-flight. In the thermal region an additional width equal to the mean decay time for the delayed emission of thermal neutrons from the source was added. Although the true effect of the delayed emission is more complex, this was considered to be the best approximation. When the effect of the resolution function on the measurements was considered, a triangular shape was always assumed. Although the true shape was quite complex and varied, it was always roughly triangular in shape and this was considered to be the best simple approximation. When a resolution triangle is indicated on a curve a width equal to the sum of the first three factors mentioned above is shown. The 3.7 percent effect and the delayed emission effect should thus be added to the width indicated for analysis.

THE EFFECT OF THE RESOLUTION WIDTH

When the timing is set for a measurement on neutrons of time-of-flight t_1, the effect of a triangular resolution function of width $2a$ will be to make the actual region of measurement lie between (t_1-a) and (t_1+a). In a measurement of the intensity distribution function from the source, I, or of the transmission function of a sample, T, the resolution width will have no effect only if these quantities are constants. When I and T are smoothly increasing or decreasing functions of the time of flight of the neutrons, there will be a distorting effect which may be expressed as a change in I or T at the point t_1. It is also permissible to regard this effect as one of changing the effective weighting over the resolution function to give the true value of I or T for a slightly different time of flight $(t_1+\alpha)$ where $|\alpha|<a$. This latter method has seemed preferable for the analysis in this paper.

If both I and T may be approximated by exponentially increasing or decreasing functions between (t_1-a) and (t_1+a) and $\Delta I/I$ and $\Delta T/T$ are the fractional changes in I and T between (t_1-a) and (t_1+a), it may be shown that α is approximately given by

$\alpha_1=(a/24)(\Delta I/I)$ for a measurement of I,
$\alpha_2=(a/24)(\Delta T/T+2\Delta I/I)$ for a measurement of T.

Since these fractional changes are usually small as compared with unity, the effective timing shift is usually quite small and is not corrected for in the analysis of the data.

When I or T pass through a sharp maximum or minimum, the averaging effect changes the measured value by an amount proportional to the curvature of the function and the square of the resolution width. A correction for this effect has been made only in the case of the cadmium resonance where a numerical integration method was employed as described below.

EXPERIMENTAL PROCEDURE

A. Intensity Measurements

After the cyclotron had been running stably for a period of time the modulator was turned on. The desired timing cycle was set and the desired cyclotron on-width and detector on-width set with respect to the 20-kilocycle oscillator. Then the number of counts coming in the timed interval was recorded using a standard number of total or untimed counts (taken with the same counter) to define the counting interval. In this manner the ordinate of the intensity *vs.* time-of-flight curve was referred to the total area under

the curve, thereby automatically eliminating any drifts that would take place. In the intensity or open-beam measurement the series of timed intensity values obtained in this manner provides all the data necessary to give the intensity *vs.* time-of-flight curve of the neutron distribution emerging from the paraffin source.

B. Transmission Measurements

In making transmission measurements with a neutron source of constant strength it is necessary only to count for *equal intervals of time* with the sample in the beam ("in" count) and with no sample in the beam ("out" count). The ratio of the two counts then gives the experimental value of the true transmission of the sample. When a source of varying intensity is employed the equal intervals of *time* are replaced by equal "intervals" of *neutron production* at the source. To measure equal intervals of cyclotron neutron production an extra BF_3 counter situated in the cyclotron enclosure was used as a monitor. In order to establish a procedure for using this extra "monitor," however, the factors involved in possible alternative procedures were examined. It should first be noted that the procedure of adjusting the counting intervals to that necessary to obtain a standard number of total detector counts as was employed in making the intensity *vs.* time-of-flight measurements will give only a *relative* transmission value when the ratio of the timed counts for the in and the out runs is taken. This is because the counting rate for the total or "untimed" counts with the sample in the beam is reduced by a factor equal to the average transmission of the sample for the particular total neutron flux distribution involved. Thus if this method were used it would also be necessary to determine the factor which would convert the *relative* transmission values to an absolute basis.

A direct method of obtaining the proper counting intervals would be to use the interval required to obtain a standard number of monitor counts as a reference as the monitor counting rate is not affected by the position of the sample. The ratio of the timed counts with sample in to that with sample out counting for intervals of equal monitor counts would then give the transmission directly. This procedure was not employed, however, because of the disadvantage that two counters are now involved and any drifts in their relative efficiencies between an in and an out run would directly introduce an additional error in the result. In the intensity measurements this effect was eliminated by comparing the number of timed counts to the total counts on the *same* counter. It was desired to retain this feature in the transmission measurements, if possible, so the procedure described below was finally adopted.

After the desired time-of-flight had been set, the out measurement was made by recording the number of timed counts q_1 and the number of monitor counts Q_3 obtained for a standard number of total detector counts Q_1. Similarly for an in run the number of timed counts q_2 and the number of monitor counts Q_4 were recorded for a standard number of total detector counts Q_2. Although Q_1 and Q_2 were in general chosen differently according to the reasoning discussed below, the value of Q_1 was the same for all out runs and Q_2 was the same for all in runs. The ratio q_2/q_1 gives a value proportional to the transmission at the point. Using the monitor counts as a reference the transmission, T, is given by $T=(q_2/q_1)(Q_3/Q_4)$. Since the ratio (Q_3/Q_4) is subject to the objection discussed above, however, the monitor ratio was first averaged over the entire run before it was applied as a correction factor to convert the relative transmission values to an absolute basis. The averaging effect and statistical accuracy introduced by a long series of alternating in and out runs thus minimizes the errors introduced in determining the monitor ratio such that the final uncertainty in a transmission value is almost entirely dependent on the uncertainties in the ratio (q_2/q_1). Since q_1 and q_2 are not affected by drifts in the counter efficiency, this freedom from the effect of drifts in counter sensitivity has largely been retained in the transmission measurements.

SAMPLES—GENERAL CONSIDERATIONS

In choosing the samples, two effects have to be taken into consideration. First, the statistical accuracy in determining the points, and, second, the resolution of the apparatus. When the transmission is a slowly varying function of the time-of-flight, the effect of the resolution of the apparatus is small and will not influence the

choice of the sample; so, in this region of a transmission curve, the sample which will give the best statistical accuracy should be used.

A relation may be obtained to give as a function of T, the transmission of the sample, the statistical uncertainty of the cross section for a fixed total counting time, t. The effect of the timed counts alone is considered in the analysis below.

Let N=counts in time t with sample out of the beam ("out position"); then NT=counts in time t with sample in the beam ("in position").

Let X=fraction of total interval t devoted to the in position; then

$N_1=XNT$=counts received for in position,

$N_2=(1-X)N$=counts received for out position,

$\alpha=\Delta N_1/N_1=1/(XNT)^{\frac{1}{2}}$

=fractional uncertainty in N_1,

$\beta=\Delta N_2/N_2=1/[(1-X)N]^{\frac{1}{2}}$

=fractional uncertainty in N_2,

$T=N_1/N_2[(1-X)/X]^{\frac{1}{2}}$

=transmission of the sample,

$$\frac{\Delta T}{T}=(\alpha^2+\beta^2)^{\frac{1}{2}}=\frac{1}{(NT)^{\frac{1}{2}}}\left[\frac{1}{X}+\frac{T}{(1-X)}\right]^{\frac{1}{2}}$$

=fractional uncertainty in T.

$T=\epsilon^{-n\sigma}$,

σ=cm^2/atom of the type considered,

$\sigma=-(1/n)\log T$,

n=atoms/cm^2 in the beam,

$$\frac{\Delta\sigma}{\sigma}=\left|\frac{\left(-\frac{1}{n}\frac{\Delta T}{T}\right)}{\left(-\frac{1}{n}\log T\right)}\right|=\frac{-\Delta T}{T\log T}=\phi(X,T).$$

To make $\phi(X, T)$ a minimum with respect to X the term $[1/X+T/(1-X)]$ in $\Delta T/T$ must be made a minimum. This gives

$X=1/(1+\sqrt{T})$ for $\phi(X, T)$ a minimum.

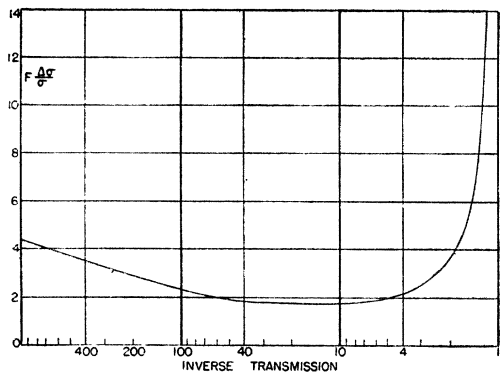

FIG. 5. Statistical error function. As a guide in choosing the optimum sample thickness this curve gives the relative statistical uncertainty in a cross section measurement as a function of the reciprocal of the transmission of the sample for a fixed counting time.

Then $\Delta T/T=(1+\sqrt{T})/(NT)^{\frac{1}{2}}$ and we obtain

$$\left(\frac{\Delta\sigma}{\sigma}\right)_{X\,\min}=\frac{-(1+\sqrt{T})}{(NT)^{\frac{1}{2}}\log T}=\frac{F(T)}{\sqrt{N}}. \qquad (1)$$

The function $F(T)=-(1+\sqrt{T})/(T^{\frac{1}{2}}\log T)$ has been plotted in Fig. 5. It is seen to have an extremely broad and flat minimum which, for practical purposes, is constant between about $T=0.01$ and $T=0.25$. Solving for the value of T at the minimum gives

$$-\log\sqrt{T}=(1+\sqrt{T})$$

as the relation to be solved. This gives

$$T=e^{-2.556}=0.0761$$

from which

$$F_{\min}(T)=1.79.$$

The effect of choosing X slightly different from the optimum value $X=1/(1+\sqrt{T})$ is also not critical in its effect on the final uncertainty. In practice X would be chosen as some convenient value near the optimum value.

Near a resonance point the transmission varies rapidly as the energy of the neutron approaches the resonance energy. The apparatus effectively averages the transmission over a time interval Δt where the efficiency of detection approximately follows a simple triangle law. If the Breit-Wigner one-level formula is assumed to hold for the cross section in the vicinity of the resonance point, the

predicted experimental transmission will be given by

$$T_{\text{exp}} = \int_{t-(\Delta t/2)}^{t+(\Delta t/2)} f(t) \times \exp\left\{-n\sigma_0(E_0/E)^{\frac{1}{2}} \Big/ \left[1+\left(\frac{E-E_0}{\Gamma/2}\right)^2\right]\right\} dt, \quad (2)$$

where

$f(t)$ is the normalized triangular resolution function,
σ_0 is the actual value of the cross section at exact resonance,
Γ is the width of the nuclear resonance line,
n is the number of absorbing atoms per square centimeter.

The predicted experimental value of the cross section at the maximum will be given by

$$\sigma_0' = -(1/n) \log T_{\text{exp}}. \quad (3)$$

Samples for Investigating Resonances

Since the experimental data should give some quantitative indication of the actual value of the cross section at the peak of the resonance curve, the number of atoms of absorbing material per square centimeter should not be large. The thicker the sample, the larger the correction factor will have to be in order to obtain the actual cross section at the peak from the observed cross section at the peak. This effect can be seen very easily if the problem is simplified by assuming that the cross section rises sharply from zero to a value σ at a time of flight t_0, is constant between t_0 and t_0+a, and then drops again to zero. If the resolution width is twice the width of this idealized line and the resolution efficiency is assumed to be constant over the interval $2a$, then the predicted minimum experimental transmission will be

$$T_{\text{exp}} = \tfrac{1}{2}[1+e^{-n\sigma}] = \exp(-n\sigma_{\text{exp}}). \quad (4)$$

From this equation it is seen that if $n\sigma$ is very small, then $\sigma_{\text{exp}} = \sigma/2$, but if $n\sigma$ becomes very large, then $n\sigma_{\text{exp}} \rightarrow \log 2$. In this simplified case the best predicted experimental value that could be obtained would be $\frac{1}{2}$ the actual value of the cross section at the maximum and as the number of atoms/cm^2 was increased the experimental cross section would approach the relation $1/n \log 2$, which is not related to σ.

Therefore, thin samples should be used in order to have the experimental value of $n\sigma_{\text{exp}}$ as sensitive as possible to variation in the actual value of $n\sigma$. The correction due to the resolution of the apparatus should also be kept small because of uncertainties in the knowledge of the exact resolution function to be used due, for example, to the small uncertainty in the fundamental timing width settings. Taking both the statistical error and the resolution error into consideration, the transmission of the sample at resonance should be about 0.3 to 0.5, this being near the upper end of the flat part of the error curve of Fig. 5.

In the cadmium measurements, two different samples of rolled Cd were used. The main measurements used a sample of 43.3 mg/cm^2 while supplementary measurements employed a 219 mg/cm^2 sample.

In the boron measurements four different samples were used because of the large range of cross-section values to be studied. In the region where the cross section was low, two thick samples of B_2O_3 were used. To prepare these samples the B_2O_3 was baked for 48 hours at 140°C to make sure that all the water was removed. The dry B_2O_3 was then packed tightly in aluminum containers to give 1.092 g/cm^2 of B_2O_3 and 0.418 g/cm^2 of aluminum for one and 2.464 g/cm^2 B_2O_3 and 0.418 g/cm^2 of aluminum in the other.

For lower energies where the cross section was higher, a thinner sample was desired so another sample containing 0.310 g/cm^2 of B_2O_3 and 0.418 g/cm^2 of aluminum was prepared in a manner similar to the others.

For the lowest energies studied as a further check on the procedure, a third sample was used which consisted of several layers of Pyrex glass totaling 0.965 g/cm^2. Analysis of this type of glass has shown that it contains 12.9 percent B_2O_3, the remaining part being mainly SiO_2. The consistency of the results with the three different samples is a good check on all the samples as the regions studied always overlapped considerably.

THE SLOW NEUTRON ENERGY DISTRIBUTION FROM THE PARAFFIN SOURCE SLABS

The exact form of the slow neutron distribution from a paraffin source is of considerable interest

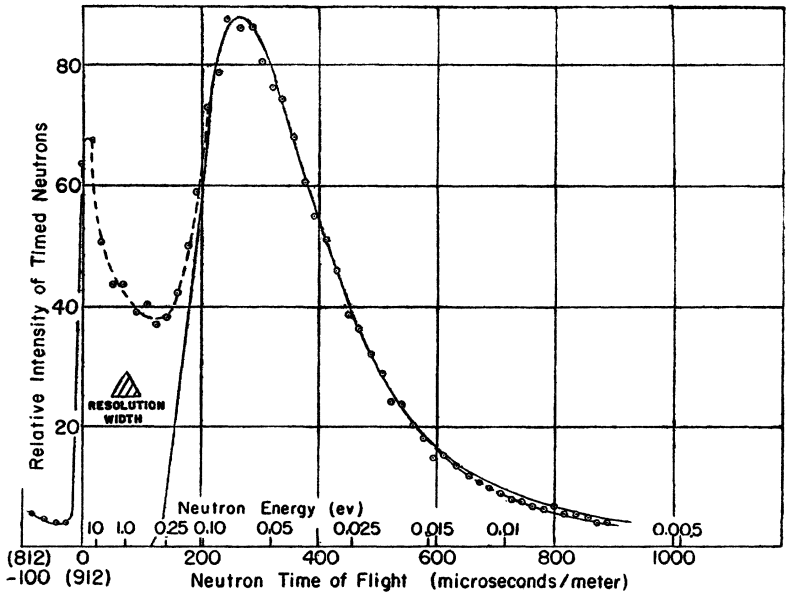

FIG. 6. The slow neutron distribution from the "thin" paraffin "source" slab. (2.6 cm thick paraffin in a box of $\frac{1}{4}$" thick plywood.) O = experimental curve. — = v^4 theoretical curve for 430°K.

as the mechanism of the establishment of thermal equilibrium between the neutrons and the paraffin is involved. Since this apparatus is particularly suited to such measurements the distributions from two source slabs were studied. This investigation was carried out to determine the shape of the emerging energy distribution also as an indication of the relative intensities to be expected in making cross-section measurements for different neutron times of flight. As a result of these and other intensity measurements, the standard source slab was chosen as one containing 2.6 cm thickness of paraffin in a box of $\frac{1}{4}$-inch thick plywood. As a "thick source" for these measurements, a 6.2-cm thickness of paraffin in a box of $\frac{1}{4}$-inch thick plywood was used.

The results of the measurements on these sources are given in Figs. 6 and 7. The source-detector distance employed was 5.4 meters and the cyclotron and detection on-time widths were both 100 microseconds. For the thin source a 5000-microsecond cycle was used and for the thick source an 8000-microsecond cycle was used to decrease the relative intensity of neutrons overlapping from previous cycles. In Figs. 6 and 7 the results have been corrected for the dead time and delayed thermal emission effects and the results reduced to a one-meter basis. In each case the approximate number of timed counts taken in obtaining a point may be obtained by multiplying the ordinate by 160. The uncertainty in the value of the timed counts is best shown, however, by the magnitude of the deviations of the points from a smooth curve.

The value of the dead time correction is shown in Fig. 3 to be about 35 microseconds. The delayed thermal emission from these slabs has been discussed above and is shown in Fig. 4. The effective source thicknesses were also discussed at that time.

Theoretical Considerations

The distributions in Figs. 6 and 7 are well matched by Maxwellian type curves of a corrected form for temperatures somewhat above the paraffin temperature. The expected form of the curves may be seen from the following discussion.

If it is assumed that the neutrons in the paraffin source are in complete thermal equilibrium with the paraffin, the number with velocities between v and $v+dv$ will be proportional to

$$N_0(v)dv = v^2 \exp(-mv^2/2kT)dv, \qquad (5)$$

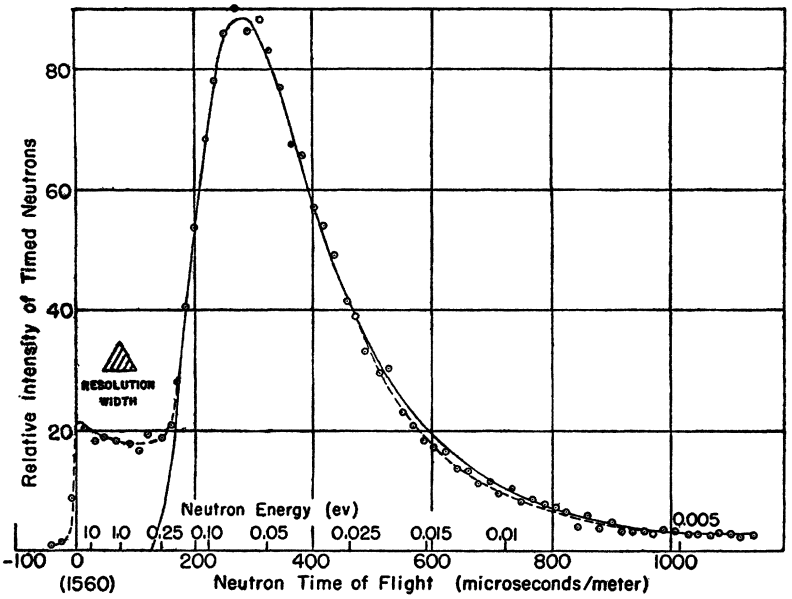

FIG. 7. The slow neutron distribution from a "thick" paraffin "source" slab. (6.2 cm thick paraffin in a box of $\frac{1}{4}$" thick plywood.) O = experimental curve. — = v^4 theoretical curve for 390°K.

where T here is used to represent the absolute temperature. If a constant mean free path is assumed, this density function will also be maintained for the neutrons emerging from the paraffin. The flux distribution, however, will contain an extra v factor to give a v^3 type distribution. Since the detector employed utilizes the $B(n, \alpha)$ reaction which is proportional to $1/v$, and the counter efficiency is always small enough to maintain this efficiency relation, the velocity distribution of neutrons detected by the BF_3 counter should be the same as $N_0(v)$.

When some parameter ϕ, other than v, is used to express the form of the distribution, we have, considering only absolute magnitudes,

$$F(\phi)d\phi = N_0(v)dv = [dv/d\phi N_0(v)]d\phi. \quad (6)$$

In these measurements equal intervals of time-of-flight, t, of the neutrons over a path of length, l, are used to give

$$F(t)dt = [N_0(v)dv/dt]dt = v^2/1N_0(v)dt,$$

or

$$F(t) = C_1 v^4 \exp(-mv^2/2kt)$$
$$= C_2 t^{-4} \exp(-ml^2/2kTt^2). \quad (7)$$

It is thus seen that the form of the predicted experimental curve should be of the v^4 or t^{-4} variety due to the above factors. This curve will thus correspond in shape neither to the neutron density, v^2, or flux, v^3, distributions from paraffin. It may easily be shown however that the value of the ordinate of the curve at any point corresponds to the *flux* distribution from paraffin expressed in equal logarithmic or fractional intervals of any of the parameters such as velocity, energy, or time-of-flight. The value of the ordinate thus corresponds to a dimensionless representation of the *flux* distribution from the paraffin. It should be noted that this is true independent of the form of the distribution function.

After the correction has been made for the delayed emission of thermal neutrons from the paraffin, the true distribution should differ from Eq. (7) for several reasons. The first of these is the fact that the mean free path of slow neutrons in paraffin continuously decreases as the energy decreases or the time of flight increases. This has the effect of making it easier for the faster neutrons to escape and thus has an effect which may roughly be described as an additional v^α factor where α is small and positive.

The second reason has to do with the fact that the neutrons initially are of several Mev energy and are slowed by successive collisions in the

paraffin. Since some of these "cascading" neutrons of all energies escape from the paraffin before reaching thermal equilibrium, a high energy tail above the thermal region will be added and a contribution to the thermal energy region will again be present which will asymmetrically favor the high energy side of the distribution. It may be noted that the existence of such a tail was shown experimentally in the first velocity selector experiments of Dunning *et al.*[5]

For a thick paraffin source the probability is small that a cascading neutron will escape after a given collision before making another. It may be shown theoretically that in such a case, in a region of constant mean free path, the flux distribution should be constant for equal logarithmic intervals of the measuring parameter. For thinner sources the curve above the thermal region should be a decreasing function of the time-of-flight where the negative exponent of t is proportional to the probability that a cascading neutron will escape immediately after a given collision. For the thick source where this probability is small the curve, Fig. 7, is nearly flat above the thermal region. For the thin source, Fig. 6, the intensity drops rapidly as the thermal region is approached. In both cases there will be a contribution of the cascading neutrons to the thermal region which will be more complicated than the corresponding contribution above the thermal region.

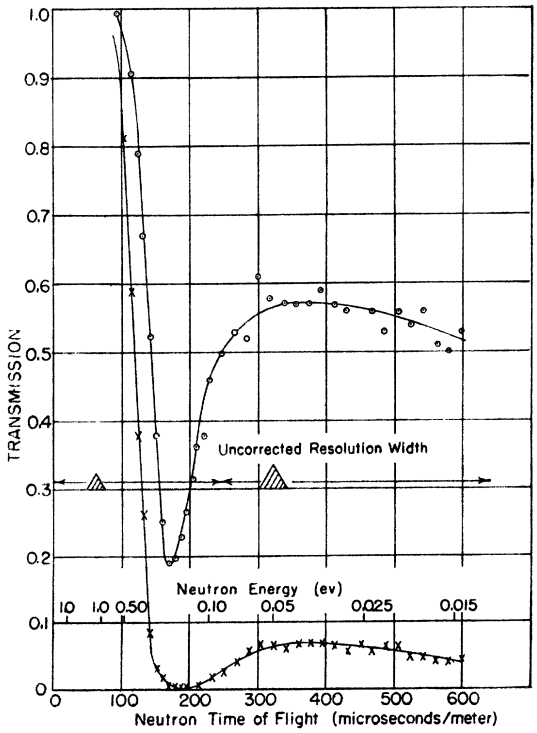

FIG. 8. Cadmium transmission curves. O = 43.3 mg/cm² Cd sample. X = 219 mg/cm² Cd sample.

The third factor which will cause the observed distribution to differ from Eq. (7) involves the mechanism of energy exchange between the neutrons and the paraffin. At thermal energies the quantum effects associated with the paraffin structure limit the probability that a low energy neutron will undergo a collision involving only a small change in energy. This has the effect of requiring a very large number of collisions to approach thermal equilibrium closely. Before this occurs many of the thermal neutrons, depending on the emission delay time, will escape in only partial thermal equilibrium and the high energy side of the distribution will again be emphasized.

Since the thermal distributions, Figs. 6 and 7, would be expected to favor higher energy neutrons relative to a curve of the form of Eq. (7) for the temperature of the paraffin source, it was considered to be of interest to see how well it could be matched by a curve of this type for a slightly higher temperature. The curve of Fig. 6 is seen to be in excellent agreement with the theoretical curve for 430°K while Fig. 7 is well matched by a theoretical curve for 390°K. These correspond, respectively, to increases of 43 and 30 percent above the absolute temperature of the paraffin slabs.

CADMIUM RESONANCE ABSORPTION

The results of the cadmium absorption measurements are given in Figs. 8 and 9. The distance employed for the time-of-flight measurements in this case was 5.4 meters with the standard thin paraffin source slab. Cyclotron and detection on-time intervals of 50 microseconds each were used for times-of-flight of less than 240 microseconds/meter where the resolution effects would be serious. For times-of-flight greater than 240 microseconds/meter the intensity and resolution functions change slowly so on-times of 100 microseconds each were employed. All data were corrected for the over-all dead time.

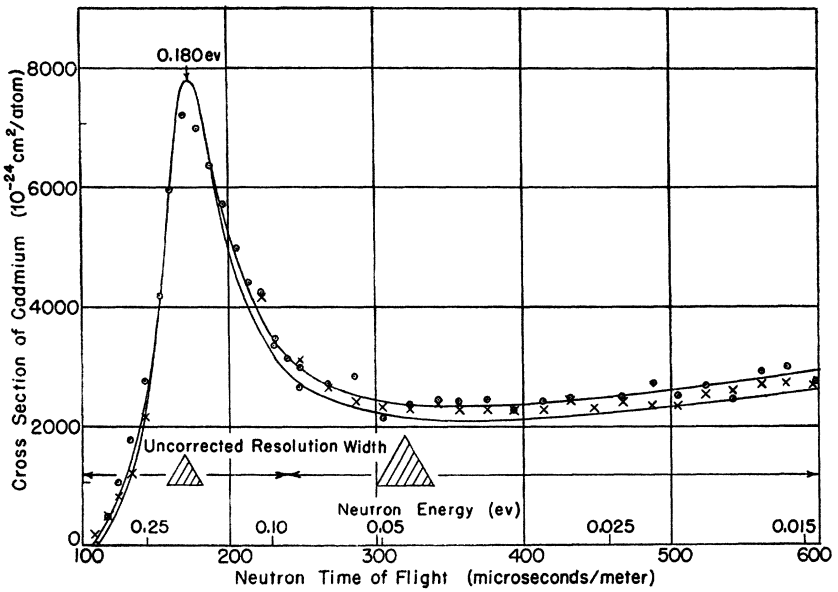

FIG. 9. Cadmium resonance cross section curve. This shows the total slow neutron cross section of Cd as a function of the time-of-flight of the incident neutrons. O = experimental points for a 43.3 mg/cm² sample. X = experimental points for a 219 mg/cm² sample. — = theoretical curves for $E_0 = 0.180$ ev; $\sigma_0 = 7800 \times 10^{-24}$ cm²/atom; $\Gamma = 0.114$ ev—upper curve; $\Gamma = 0.108$ ev—lower curve.

The delayed thermal emission correction of 45 microseconds was not applied suddenly but was gradually added over the region between 700 and 1500 microseconds for 5.4 meters or 125 and 265 microseconds on the one-meter basis. The gradation was chosen by reference to Fig. 6 from which the ratio of thermal to cascading neutrons can be estimated with fair accuracy. Since the total correction amounts to only 8.3 microseconds, and the uncertainty in the correction factor is certainly much less than this, the total error due to this factor is probably less than 2 microseconds/meter.

For a single sample which could be used over the entire region of interest a 43.3 mg/cm² sheet of rolled Cd was employed. To give supplementary information near the "transmission edge" and for energies below the peak a 219 mg/cm² sample was used. The transmission curves for these two samples are shown in Fig. 8. The cross sections corresponding to these measured transmissions are given in Fig. 9 together with two reference Breit-Wigner one-level curves.

The procedure employed in matching the experimental points in Fig. 9 to a best fitting theoretical curve was one of trial and error. In the region above 240 microseconds/meter the effect of the resolution is negligible so these values were considered to be reliable within the accuracy of the measurement. In the region of the peak, however, the effect of the resolution width is to make the measured transmission greater than the true transmission by averaging the "true transmission" curve over a region given by the resolution function. In the region of the peak the resolution width was taken as 30 microseconds/meter including the cyclotron and detector on-times, the effect of the counter length, and a partial thermal delay width.

A numerical integration near the peak employing a theoretical Breit-Wigner transmission curve and a 30 microsecond/meter resolution width indicated that the correction at the peak should be about 8 percent. Thus the value of σ_0 chosen for the calculation was $\sigma_0 = 7800 \times 10^{-24}$ cm²/atom. Since the asymmetric effect of the $1/v$ factor in the Breit-Wigner formula moves the maximum of the cross-section curve to the right of the resonance time-of-flight (Fig. 9), the best value of the resonance time-of-flight was determined by a matching process to be $t_0 = 170$ microseconds/meter corresponding to $E_0 = 0.180$ ev.

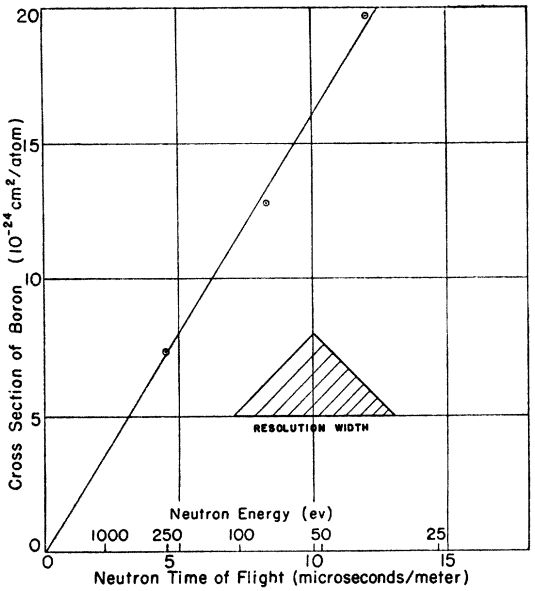

FIG. 10. Boron cross section curve for higher energies. O = experimental points. — = straight-line relation $\sigma = 118E^{-\frac{1}{2}} \times 10^{-24}$ cm^2/atom.

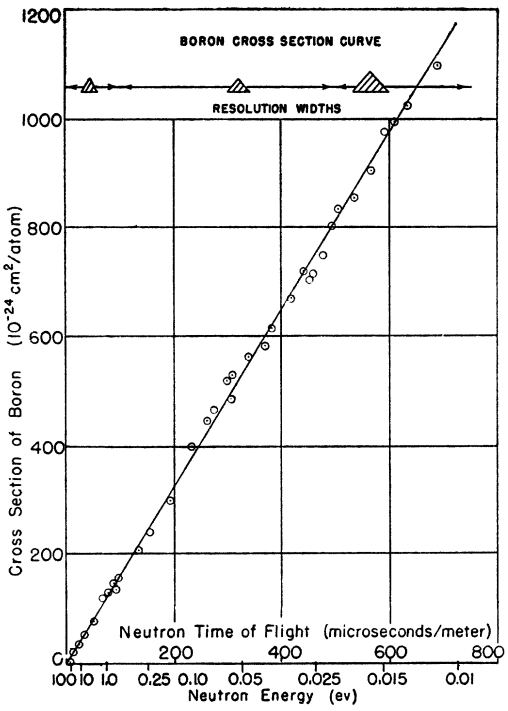

FIG. 11. Boron cross section curve. O = experimental points. — = straight-line relation $\sigma = 118E^{-\frac{1}{2}} \times 10^{-24}$ cm^2/atom.

In Fig. 9 close matching theoretical curves for two values of Γ have been shown. These indicate the best value of Γ and also show the sensitivity of the agreement for times of flight above 240 microseconds/meter.

Considering all the possible sources of error which may be involved in such measurements as described above, the final results for Cd may be stated as follows:

$$\sigma_0 = (7800 \pm 800) \times 10^{-24} \text{ cm}^2/\text{atom},$$
$$\sigma_{\min} = (2300 \pm 150) \times 10^{-24} \text{ cm}^2/\text{atom near } 0.04 \text{ ev},$$
$$\Gamma = (0.112 \pm 0.006) \text{ ev},$$
$$E_0 = (0.180 \pm 0.008) \text{ ev}.$$

The agreement of the experimental results with the Breit-Wigner curve of Fig. 9 is very gratifying as such an extended experimental comparison has not been made for this theory before. Since Cd is used as a standard filtering material for slow neutron measurements an accurate knowledge of the resonance parameters should prove useful.

In the above analysis no effort was made to assign the effect to a single isotope and an average value for normal Cd was given. If it is assumed that the capture cross section is caused by an odd isotope whose abundance is 13 percent, the effective cross section becomes $\sigma_0 = 60{,}000 \times 10^{-24}$ cm^2/atom. This gives $\Gamma_N = 1.86 \times 10^{-3}$ ev or 0.62×10^{-3} ev depending on the angular momentum of the resulting nucleus.

BORON RESULTS

The results of the measurements with the boron absorbers are given in Figs. 10 and 11. The samples employed have already been described above. The measurements were taken with a source-detector distance of 5.2 meters for some of the points and 5.4 meters for the others, always using the standard thin paraffin source slab. In all cases the dead time correction was made and the delayed thermal emission correction was applied as discussed above. The times of flight were then reduced to a one-meter basis for plotting.

For measurements above the Cd cut-off region a total cycle period of 1000 microseconds was used. For the highest energy measurements shown in Fig. 10 the cyclotron and detection on-time intervals were reduced to about 15 microseconds each to give a total resolution width of

about 6 microseconds/meter. For the measurements below 100 microseconds/meter the total resolution width was 20 microseconds/meter plus 3.7 percent of the time-of-flight due to the counter length.

For the remainder of the measurements a 5000-microsecond cycle was used with cyclotron and detection, on-time widths of 100 microseconds each below 500 microseconds/meter and 150 microseconds each above 500 microseconds/meter. In calculating the total resolution width above 200 microseconds/meter the delayed thermal emission width of 45 microseconds and the 3.7 percent effect due to the counter length must be added to the sum of the cyclotron and detection on-time intervals.

The results for the main part of the boron measurements are shown in Fig. 11 and it is seen that, over the region studied, the experimental points are well matched by the $1/v$ relation

$$\sigma_B = 118\times10^{-24}E^{-\frac{1}{2}}\ \text{cm}^2/\text{atom},$$

where E is expressed in electron volts. Since it was considered desirable to extend the measurements to higher energies, the resolution was reduced to a minimum and a 2.464 g/cm^2 sample of B_2O_3 was used. Since the scattering cross sections of oxygen and aluminum are an important fraction of the total cross section for energies above 100 ev, it is probably only fortuitous that the straight lines formed by the points pass through the origin rather than being shifted upwards or downwards. Also it is seen that the resolution width, although reduced to a very small absolute value, is not small compared to the measured times-of-flight. The fact that the intensity and the transmission are relatively slowly varying functions of the time of flight in this region probably makes the points in Fig. 10 more significant on a time-of-flight basis than the rapid rate of change of the energy scale would indicate.

The results were corrected for the effect of the oxygen and aluminum present for the B_2O_3 samples and the SiO_2 present in the Pyrex samples. For oxygen the value of 4.1×10^{-24} cm^2/atom was used[11] and for silicon the value 2.5×10^{-24} cm^2/atom. This value of the cross section for silicon was used rather than a value for SiO_2 because the measured cross sections of SiO_2 are usually too low because of structural effects which should not be important in Pyrex.[11,12] For aluminum the cross section was assumed to be 1.5×10^{-24} cm^2/atom. Small uncertainties in these corrections are not serious over most of the region because of the large boron cross section. They become most important for the values in Fig. 10. It should also be noted in this respect that the effect of a constant cross section is only to displace the straight line vertically without changing its slope.

These time-of-flight measurements give a clear experimental check on the $1/v$ law for boron within the experimental accuracy over a large energy range. It is fortunate that the results do demonstrate that boron follows a $1/v$ law as the interpretation of a great deal of experimental work has been based on this assumption.

The results of these measurements together with an estimate of the over-all uncertainty present may be given as:

$$\sigma_B = (118\pm4)E^{-\frac{1}{2}}\times10^{-24}\ \text{cm}^2/\text{atom},$$

where E is the neutron energy in electron volts. This equation gives directly the $1/v$ proportionality factor for boron and should be of value in resonance-detector measurements for determining the positions of the energy levels without the necessity of making the customary comparison with thermal neutrons, of somewhat undefined effective energies. Since the lack of this knowledge has been one of the major sources of uncertainty in previous energy determinations, this should permit re-examination of earlier measurements.

The writers wish to express their appreciation of the interest taken in this problem by Professor J. R. Dunning, who originally suggested the problem and without whose active interest and stimulating discussions the work could not have been carried out. The Ernest Kempton Adams Fellowship Fund has aided materially in providing the special equipment for this work.

[11] Henry Carroll, Phys. Rev. **60**, 702 (1941).

[12] Whitaker, Bright, and Murphy, Phys. Rev. **57**, 551 (1940).